Neuron
Article

SV2 Acts via Presynaptic Calcium to Regulate Neurotransmitter Release

Qun-Fang Wan,[1,4] Zhen-Yu Zhou,[1,4] Pratima Thakur,[1] Alejandro Vila,[1,2] David M. Sherry,[3] Roger Janz,[1,2,*] and Ruth Heidelberger[1,2,*]
[1]The Department of Neurobiology and Anatomy, University of Texas Medical School at Houston, Houston, TX 77030, USA
[2]The Graduate School of Biomedical Sciences, University of Texas Health Science Center at Houston, Houston, TX 77030, USA
[3]University of Oklahoma Health Sciences Center, Department of Cell Biology and Oklahoma Center for Neuroscience, Oklahoma City, OK 73104, USA
[4]These authors contributed equally to this work
*Correspondence: roger.janz@uth.tmc.edu (R.J.), ruth.heidelberger@uth.tmc.edu (R.H.)
DOI 10.1016/j.neuron.2010.05.010

SUMMARY

Synaptic vesicle 2 (SV2) proteins, critical for proper nervous system function, are implicated in human epilepsy, yet little is known about their function. We demonstrate, using direct approaches, that loss of the major SV2 isoform in a central nervous system nerve terminal is associated with an elevation in both resting and evoked presynaptic Ca^{2+} signals. This increase is essential for the expression of the *SV2B*$^{-/-}$ secretory phenotype, characterized by changes in synaptic vesicle dynamics, synaptic plasticity, and synaptic strength. Short-term reproduction of the Ca^{2+} phenotype in wild-type nerve terminals reproduces almost all aspects of the *SV2B*$^{-/-}$ secretory phenotype, while rescue of the Ca^{2+} phenotype in *SV2B*$^{-/-}$ neurons relieves every facet of the *SV2B*$^{-/-}$ secretory phenotype. Thus, SV2 controls key aspects of synaptic functionality via its ability to regulate presynaptic Ca^{2+}, suggesting a potential new target for therapeutic intervention in the treatment of epilepsy.

INTRODUCTION

SV2 proteins are a group of homologous integral membrane proteins found on secretory vesicles that undergo regulated release (Bajjalieh et al., 1992; Buckley and Kelly, 1985; Feany et al., 1992). They have 12 transmembrane domains and are members of the major facilitator superfamily of membrane transporter proteins (Janz et al., 1998; Saier et al., 1999). In mammals, the three isoforms, SV2A, SV2B, and SV2C, are each encoded by a separate gene (Bajjalieh et al., 1994; Janz and Südhof, 1999). Inactivation of the gene coding for SV2A, by far the most widely distributed isoform in the mouse brain, results in early postnatal-lethal epileptic-like seizures (Crowder et al., 1999; Janz et al., 1999). In humans, SV2A has been identified as a target of levetiracetam, a highly effective drug used in the treatment of epilepsy (De Smedt et al., 2007; Lynch et al., 2004), and a reduction in SV2A has been recently reported in patients with temporal lobe epilepsy (Feng et al., 2009). SV2 proteins can also interact with botulinum neurotoxins (Dong et al., 2006, 2008; Mahrhold et al., 2006), allowing their entry into nerve terminals during exocytosis, where they exert their toxic effects.

Despite their critical role in nervous system health, the function of SV2 proteins is far from clear. While some researchers have suggested that SV2 proteins govern synaptic plasticity by regulating residual calcium (Chang and Südhof, 2009; Janz et al., 1999), others have argued that SV2 proteins act independently of changes in presynaptic calcium (Custer et al., 2006; Xu and Bajjalieh, 2001); evidence for both viewpoints is largely indirect. In addition, SV2 proteins have been suggested to act either before or after a priming step in the secretory pathway (Chang and Südhof, 2009; Xu and Bajjalieh, 2001). Unfortunately, precise elucidation of the function of SV2 proteins has been hindered by several factors, including the severe seizures and early lethality associated with the absence of the major brain isoform of SV2, SV2A. In addition, biochemical approaches have been hampered by the fact that SV2 proteins are heavily glycosylated, polytopic membrane proteins that are difficult to express functionally in recombinant systems. Physiological approaches have been hampered by the lack of a neuronal preparation that permits quantitative and simultaneous measurement of presynaptic calcium and synaptic vesicle dynamics in neurons with SV2 deficiency.

In this study, we took advantage of a neuronal preparation recently developed for the direct, biophysical study of exocytosis and presynaptic calcium in the mammalian central nervous system: the mouse rod bipolar cell (Wan et al., 2008; Zhou et al., 2006). In addition, we took advantage of the fact that SV2B is the major SV2 isoform expressed in these neurons (Wang et al., 2003) and that SV2B knockout mice are viable and do not suffer from seizures (Janz et al., 1999). This allowed us to investigate SV2 function in neurons isolated from mature, healthy animals. The only known deficit in SV2B knockout animals resides in the retina, consistent with a major role for SV2B in ribbon synapses of the rod visual pathway (Lazzell et al., 2004; Morgans et al., 2009).

We compared the presynaptic Ca^{2+} and secretory responses of rod bipolar cells acutely isolated from the retinae of adult

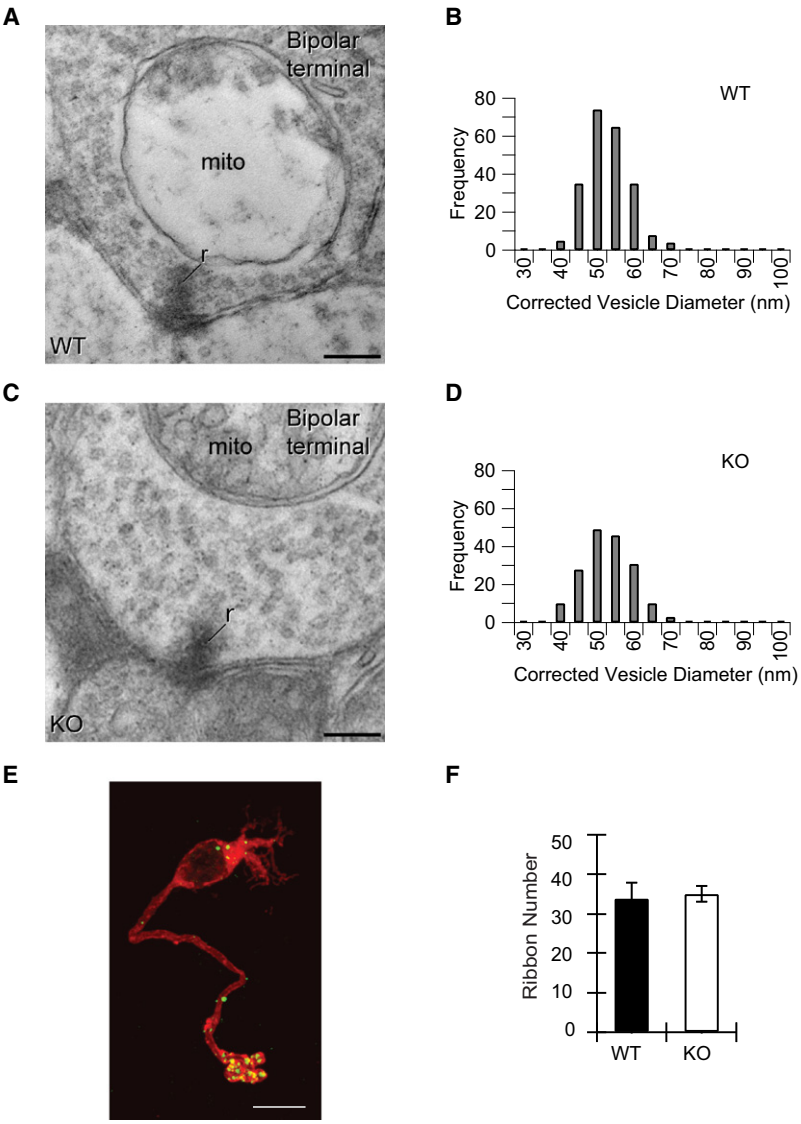

Figure 1. Absence of SV2B Does Not Affect Synaptic Architecture

(A and C) The absence of SV2B does not disrupt bipolar cell ribbon synapse ultrastructure or organization. Ribbon synapses in bipolar cell terminals of WT and *SV2B*$^{-/-}$ (KO) retina show similar ultrastructure, with short synaptic ribbons (r) attached to the presynaptic membrane and surrounded by numerous synaptic vesicles. Postsynaptic processes from amacrine or ganglion cells flank the synaptic ribbon in the normal diad organization (Dowling, 1968). Mito, mitochondrion. Scale bars, 0.2 μm.

(B and D) The distribution of synaptic vesicle diameters in bipolar cell terminals in WT and KO retina is comparable. Feret's diameter was measured from digitized electron micrographs and adjusted using Abercrombie's correction factor to adjust for systematic underestimation of the size of spherical objects in thin sections (Abercrombie, 1946).

(E and F) Loss of SV2B did not alter the number of synaptic ribbons in bipolar cell terminals. (E) Confocal fluorescence image of a freshly isolated rod bipolar cell from an *SV2B*$^{-/-}$ mouse double immunostained for the synaptic ribbon marker CtBP2 (green) and the rod bipolar cell marker protein kinase C-α (PKC-α, red). Scale bar, 10 μm. (F) The number of ribbons in terminals did not differ between WT and KO mice. The number of synaptic ribbons in WT and KO rod bipolar terminals was determined by counting the number of CtBP2-positive puncta in the terminals of rod bipolar cells positively identified as rod bipolar cells by PKC-α labeling. WT ribbon counts from Wan et. al. (2008). Error bars represent SEM.

SV2B$^{-/-}$ and wild-type mice using quantitative fluorescence measurements of presynaptic Ca^{2+} in combination with time-resolved membrane capacitance measurements (Wan et al., 2008; Zhou et al., 2006). Our data provide direct evidence that SV2B is important for the regulation of presynaptic Ca^{2+} levels and, consequently, Ca^{2+}-dependent synaptic vesicle dynamics. In addition, we identified a role for SV2B that is independent of short-term changes in presynaptic Ca^{2+} and is reminiscent of the previously described peri-priming defect (Chang and Südhof, 2009; Custer et al., 2006). Strikingly, every aspect of the SV2B knockout secretory phenotype, including the functional reduction in the rapidly releasing pool, was relieved by the restoration of presynaptic Ca^{2+} signaling to wild-type levels. Thus, not only does this SV2 protein play a key role in regulating presynaptic Ca^{2+}, but presynaptic Ca^{2+} signaling plays a key role in the expression of the SV2-deficiency phenotype.

RESULTS

SV2B Regulates Presynaptic Ca^{2+} Signaling

Previous ultrastructural analysis of conventional synapses from SV2A/B double-knockout mice has shown that the lack of SV2 proteins does not affect the formation of morphologically normal synapses or synaptic vesicles (Crowder et al., 1999; Janz and Südhof, 1999). Similarly, we found that the absence of SV2B did not alter the structure and size of synaptic vesicles or the number or length of synaptic ribbons at the ribbon-style synapses of the mouse rod bipolar cell (Figure 1 and Table S1). Neither did the absence of SV2B disrupt formation of normal synaptic connections by bipolar cells (Figure 1).

To ascertain whether SV2 proteins regulate the resting presynaptic Ca^{2+} concentration, we performed quantitative measurements of spatially averaged presynaptic Ca^{2+} in bis-fura-2-loaded terminal boutons of isolated, mature rod bipolar neurons from SV2B knockout mice (*SV2B*$^{-/-}$) and wild-type littermates (Figure 2). To control for changes in membrane potential that could alter calcium signaling, neurons were held under voltage-clamp control at −70 mV. Under these conditions, the mean spatially averaged intraterminal Ca^{2+} concentration of neurons obtained from *SV2B*$^{-/-}$ mice was 88 ± 14 nM (n = 27), compared with 35 ± 5 nM (n = 34) in wild-type (WT) littermates (p = 0.00028) (Figure 2B).

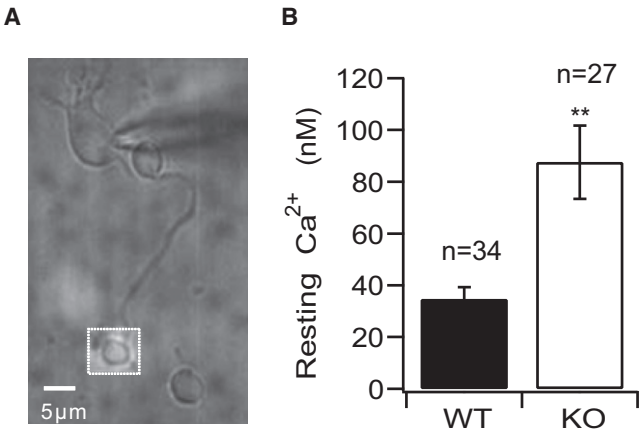

Figure 2. Absence of SV2B Is Associated with Elevated Resting Presynaptic Ca^{2+}

(A) An acutely isolated rod bipolar neuron is shown with a patch pipette on its soma. The dotted square over the terminal denotes the region from which the emitted bis-fura-2 fluorescence signal was collected.

(B) The average resting Ca^{2+} concentration in synaptic terminals held at −70 mV is significantly higher in neurons from *SV2B*$^{-/-}$ mice (KO) than WT littermates. Error bars represent SEM. **p < 0.01.

To establish whether or not SV2 proteins influence evoked Ca^{2+} signals, we applied a brief 4 Hz stimulus train to bipolar neurons from *SV2B*$^{-/-}$ and WT mice. Each pulse in the train was of a magnitude and duration sufficient to deplete the rapidly releasing pool of vesicles (Wan et al., 2008). We simultaneously monitored the spatially averaged presynaptic Ca^{2+} concentration and changes in membrane capacitance as an index of synaptic vesicle fusion (Figure 3; see also Figure S1). The average cumulative increase in presynaptic Ca^{2+} concentration was greater in *SV2B*$^{-/-}$ terminals than in WT terminals for each pulse in the train (Figure 3A). In general, the rise in presynaptic free Ca^{2+} evoked by each pulse was approximately double in *SV2B*$^{-/-}$ terminals relative to WT (Pulse 1: WT: 58 ± 16 nM, n = 13; *SV2B*$^{-/-}$: 124 ± 21 nM, n = 14; p = 0.018; Pulse 10: WT: 219 ± 50; *SV2B*$^{-/-}$: 555 ± 94 nM, p = 0.0046; Figure 3A). Taken with results from the previous section, our results provide strong evidence for a role for SV2 proteins in the regulation of both resting and evoked Ca^{2+} signaling in nerve terminals.

SV2B Regulates Synaptic Vesicle Dynamics

We next examined the extent of exocytosis evoked by the stimulus train in neurons with and without SV2B. Figure 3B presents our analysis of the cumulative capacitance change as a function of pulse number (see also Figure S1). In *SV2B*$^{-/-}$ neurons, there was a dramatic decrease in the magnitude of the first exocytotic response relative to WT neurons (*SV2B*$^{-/-}$: 2.8 ± 0.8 fF, n = 12; WT: 9.2 ± 1.5 fF, n = 13; p = 0.0015), suggesting that there is a decrease in the fusion of rapidly releasing vesicles in the absence of SV2B. This decrease was accompanied by an increase in the slope of the cumulative capacitance increase early in the pulse train ($Slope_{pulses1\text{-}3}$ *SV2B*$^{-/-}$: 3.1 ± 0.4; $Slope_{pulses1\text{-}3}$ WT: 1.2 ± 0.2; PROC Mixed analysis, p = 0.0393). This enhancement briefly converts depression in the WT to facilitation in the *SV2B*$^{-/-}$ neurons (Figures 3B and 3C). However, the maximum cumulative release was essentially identical (*SV2B*$^{-/-}$: 20.5 ± 3.8 fF, n = 12; WT: 19.9 ± 1.9 fF,

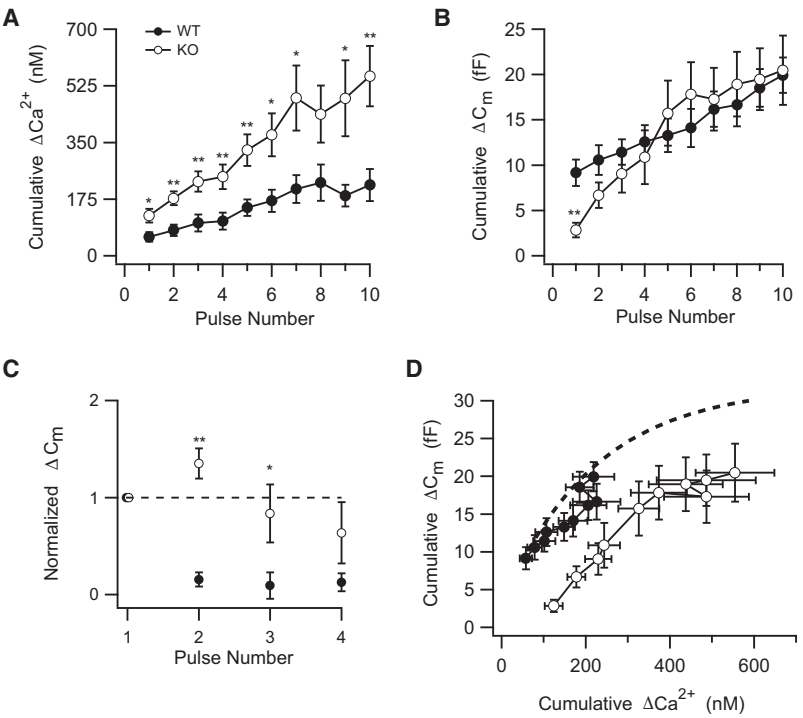

Figure 3. Absence of SV2B Is Associated with a Larger Increase in Cumulative Ca^{2+} and a Change in the Pattern of Exocytosis

(A) The mean cumulative ΔCa^{2+} concentration for each pulse in the train was higher in terminals from *SV2B*$^{-/-}$ mice (KO) relative to WT littermates. *p < 0.05, **p < 0.01.

(B) Despite greater increases in intraterminal Ca^{2+} concentration in *SV2B*$^{-/-}$ terminals, the ΔC_m increase evoked by the first pulse of the stimulus train was smaller in *SV2B*$^{-/-}$ terminals than in WT terminals, while the cumulative ΔC_m increase after the tenth pulse was similar. Furthermore, the slope of the cumulative ΔC_m during the initial three pulses of the train was steeper in *SV2B*$^{-/-}$ neurons.

(C) Facilitation precedes depression in *SV2B*$^{-/-}$ neurons but not WT neurons. The normalized ΔC_m responses evoked by the stimulus for WT rod bipolar cells (filled circles) shows a pronounced synaptic depression. By contrast, *SV2B*$^{-/-}$ (KO) neurons (open circles) exhibit facilitation that is followed by a slower rate of depression. The average ΔC_m evoked by each pulse is normalized to that of the first; only the first four responses to the train are shown.

(D) The cumulative ΔC_m with respect to the cumulative ΔCa^{2+} concentration was significantly shifted to the right in *SV2B*$^{-/-}$ compared to WT terminals. The estimated size of the shift was 7 fF. Dotted line shows the relationship predicted from Zhou et al. (2006). See also Figure S1.

Error bars represent SEM.

n = 13; p = 0.9), indicating that the total number of vesicles released by the whole train was similar between *SV2B*$^{-/-}$ and WT neurons.

Comparison of Figures 3A and 3B raised the possibility that the extent of exocytosis in *SV2B*$^{-/-}$ neurons began to approximate that of WT neurons as the relative change in cumulative Ca^{2+} concentration exceeded that of WT neurons. To evaluate this possibility, for each pulse in the train, we graphed the cumulative change in membrane capacitance as a function of the cumulative increase in presynaptic Ca^{2+} concentration. Figure 3D demonstrates that relative to WT neurons, the curve for *SV2B*$^{-/-}$ neurons was shifted to the right by ~7 fF (PROC Mixed analysis, p < 0.0001, estimated shift 7 fF). This finding could indicate that the absence of SV2B is associated with a decrease in the apparent Ca^{2+} sensitivity of release, assuming that the spatially averaged presynaptic Ca^{2+} concentration and Ca^{2+} concentration at the release site are correlated (Naraghi and Neher, 1997).

The time course for the restoration of membrane capacitance following a stimulus train also differed between *SV2B*$^{-/-}$ and WT neurons (Figure 4). *SV2B*$^{-/-}$ terminals displayed a slower average time constant for membrane recovery than WT terminals (*SV2B*$^{-/-}$: 9.5 ± 0.8 s, n = 8; WT: 4.5 ± 0.9 s, n = 12; p = 0.0015). This may reflect either a decrease in the rate of endocytosis, an increase in asynchronous release, or a combination of both. By contrast, Ca^{2+} concentration recovered to the prestimulus baseline with a time constant of a few seconds in both neurons (Figure 4: *SV2B*$^{-/-}$: 1.9 ± 0.1 s, n = 17; WT: 2.0 ± 0.2 s; n = 16; p = 0.59), indicating that other presynaptic Ca^{2+} handling mechanisms remained intact (Zenisek and Matthews, 2000).

Taken together, our data demonstrate that SV2 deficiency gives rise to both a Ca^{2+} phenotype and a secretory phenotype. The former is characterized by elevated spatially averaged resting Ca^{2+} concentration and an enhanced evoked Ca^{2+} response in nerve terminals. The latter is characterized by a decrease in the number of rapidly releasing vesicles, a decrease in the apparent Ca^{2+} sensitivity of exocytosis, an early enhancement of the secretory response evoked by a stimulus train, and a prolongation of membrane recovery.

Restoration of Presynaptic Ca^{2+} Signaling Rescues the *SV2B*$^{-/-}$ Secretory Phenotype

Several aspects of secretory vesicle dynamics are regulated by intraterminal Ca^{2+} (Heidelberger, 2001; Neher and Sakaba, 2008). We therefore asked whether we could rescue the *SV2B*$^{-/-}$ secretory phenotype by restoring resting intraterminal Ca^{2+} levels to near WT values. To this end, we clamped the resting intraterminal Ca^{2+} concentration in *SV2B*$^{-/-}$ and WT terminals via the use of a Ca^{2+}-buffered internal recording solution (solution B; Table 1). Following 2 min of dialysis with solution B, the mean intraterminal free-Ca^{2+} concentration in *SV2B*$^{-/-}$ terminals held at −70 mV was 52 ± 4 nM (n = 16), representing an ≈40% decrease from what was measured for *SV2B*$^{-/-}$ terminals using our standard recording solution (solution A; Figure 5A; 112 ± 27 nM, n = 14; p = 0.037). The mean intraterminal free-Ca^{2+} concentration in *SV2B*$^{-/-}$ neurons dialyzed with solution B was indistinguishable from that of WT terminals dialyzed with solution B (Figure 5A; $WT_{solutionB}$: 57 ± 6 nM, n = 17). With solution B, the rise in cumulative intraterminal Ca^{2+} concentration in *SV2B*$^{-/-}$ neurons evoked by the pulse train was essentially identical to that of WT neurons (Figure 6A), and the total cumulative Ca^{2+} concentration rise was reduced to

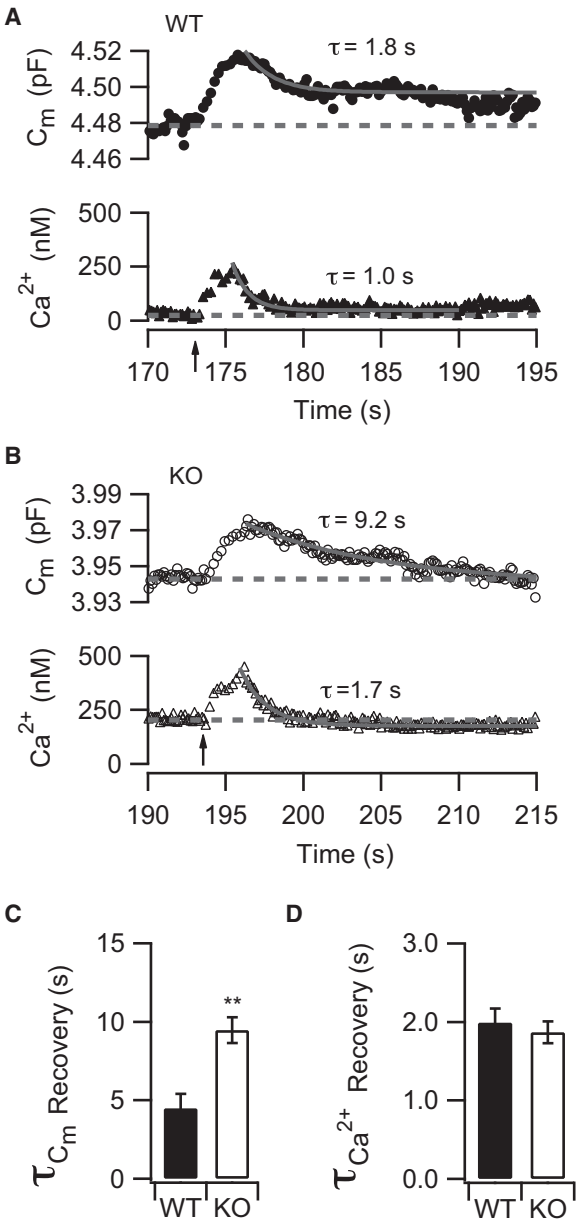

Figure 4. The Rate of Membrane Recovery Following a Stimulus Train Is Prolonged in *SV2B*$^{-/-}$ Terminals

(A and B) Typical capacitance (circles) and Ca^{2+} (triangles) responses following a pulse train in WT (filled circles) and *SV2B*$^{-/-}$ terminals (KO, open circles). Superimposed curves in (A) and (B) represent the single-exponential fit for each trace. Time constants are as indicated.

(C and D) Following the pulse train, membrane recovery was significantly slower in *SV2B*$^{-/-}$ terminals than in WT littermates (C; **p < 0.01). However, there was no difference between *SV2B*$^{-/-}$ and WT terminals in the time course of recovery of Ca^{2+} concentration to baseline following the stimulus train (D). Error bars represent SEM.

Table 1. Table of Intracellular Solutions

Solution (mM)	A	B	C	D
$CaCl_2$	0	0.05	0.3	0.15
EGTA	0.5	0.55	0.5	0.2
Calculated free EGTA	0.5	0.48	0.25	0.1
Calculated free Ca^{2+} (nM)	0	14	173	163
Measured free Ca^{2+} (nM)	0	12	241	225

312 ± 70 nM (n = 16), representing an ≈40% decrease from what was measured using our standard solution (solution A; Figure 3A). The time constant of Ca^{2+} recovery was similar between *SV2B*$^{-/-}$ and WT terminals (data not shown), as expected from our earlier findings (i.e., Figure 4D).

What happens to exocytosis in *SV2B*$^{-/-}$ terminals with a WT Ca^{2+} phenotype? We addressed this question in *SV2B*$^{-/-}$ and WT neurons dialyzed with the Ca^{2+}-defined internal recording solution described above (solution B). In contrast to what was observed previously in response to the pulse train, the average magnitude of the first capacitance jump in *SV2B*$^{-/-}$ neurons dialyzed with solution B was no longer suppressed (Figure 6B). Rather, it was indistinguishable from that of WT terminals (Figure 6B; *SV2B*$^{-/-}{}_{\text{solutionB}}$: 11.7 ± 1.8 fF, n = 16; $WT_{\text{solutionB}}$: 12.1 ± 1.8 fF, n = 17) and significantly different from *SV2B*$^{-/-}$ neurons dialyzed with solution A. In addition, there was no longer a difference in the slope of the cumulative capacitance increase as a function of pulse number for the first three points in the train (Figure 6B; Slope *SV2B*$^{-/-}{}_{\text{solutionB}}$: 3.2 ± 1.4; Slope $WT_{\text{solutionB}}$: 1.8 ± 1.0, PROC Mixed analysis, p = 0.1574), indicating that the early enhancement seen in Figure 3B may represent a Ca^{2+}-dependent process. Furthermore, with solution B, the apparent Ca^{2+} sensitivity of release for *SV2B*$^{-/-}$ neurons was no longer shifted to the right, but rather was superimposable upon that of WT neurons (Figure 6C, PROC Mixed analysis, $WT_{\text{solutionB}}$ versus $KO_{\text{solutionB}}$, p = 0.4). Thus, restoration of presynaptic Ca^{2+} signaling to wild-type patterns relieves the *SV2B*$^{-/-}$ secretory phenotype.

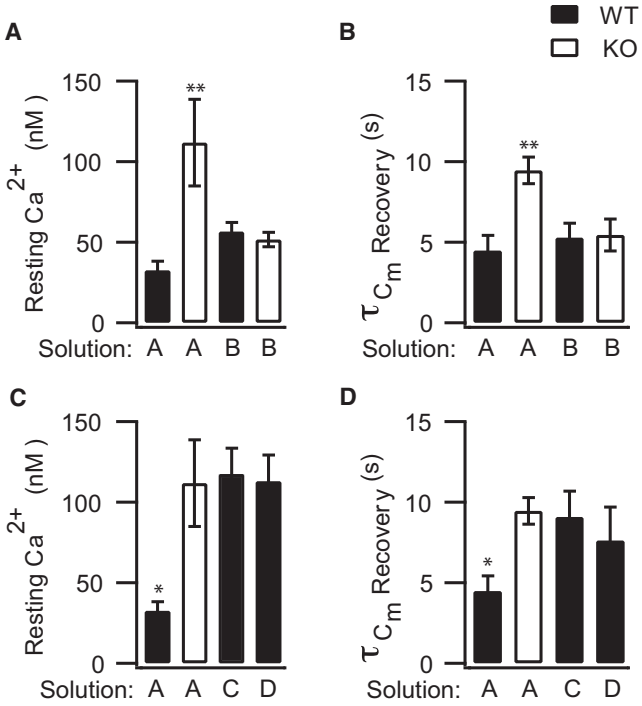

Figure 5. The *SV2B*$^{-/-}$ Membrane Retrieval Phenotype Is Sensitive to Manipulation of Presynaptic Ca^{2+}

(A and B) Lowering presynaptic Ca^{2+} concentration with solution B restores the mean rate of membrane retrieval in *SV2B*$^{-/-}$ (KO) neurons (open bar; solution B) to that of WT neurons (filled bars).

(C and D) In WT neurons, solutions C or D mimicked the KO phenotype of higher resting Ca^{2+} concentration and slower rate of membrane retrieval. Data were analyzed by one-way ANOVA followed by Dunnett's Multiple Comparisons Test. **p < 0.01, *p < 0.05.

Error bars represent SEM.

If the loss of SV2 proteins indirectly alters the time course of membrane recovery following exocytosis via an increase in presynaptic Ca^{2+} concentration, then mimicking the WT Ca^{2+} phenotype in an *SV2B*$^{-/-}$ neuron should restore the time constant of membrane recovery of *SV2B*$^{-/-}$ terminals to control values. This is precisely what we observed (Figure 5B). For example, following the pulse train, the average time constant of membrane recovery for *SV2B*$^{-/-}$ neurons was 5.4 ± 1.0 s (solution B; n = 9) compared with 5.3 ± 0.9 s for WT neurons (solution B; n = 10). Given previous results indicating that larger rises in spatially averaged Ca^{2+} concentration are associated with longer time constants of membrane recovery in bipolar neurons (von Gersdorff and Matthews, 1994; Wan et al., 2008), these results suggest that the prolonged time course of membrane recovery in *SV2B*$^{-/-}$ neurons dialyzed with our standard recording solution (solution A) may be directly attributed to the *SV2B*$^{-/-}$ Ca^{2+} phenotype.

Mimicking the *SV2B*$^{-/-}$ Ca^{2+} Phenotype in WT Neurons Does Not Reproduce the Full *SV2B*$^{-/-}$ Secretory Phenotype

If the secretory phenotype of *SV2B*$^{-/-}$ neurons is a direct consequence of the *SV2B*$^{-/-}$ Ca^{2+} phenotype, then WT neurons with an *SV2B*$^{-/-}$ Ca^{2+} phenotype should display the *SV2B*$^{-/-}$ secretory phenotype. To test this hypothesis, we manipulated the Ca^{2+} profile in WT and *SV2B*$^{-/-}$ neurons by internal dialysis with either high Ca^{2+} solution C or D; these solutions differ in the amount of free EGTA (Table 1). With either solution, ~2 min after achieving the whole-cell recording configuration, the resting Ca^{2+} in WT terminals was increased to a level similar to *SV2B*$^{-/-}$ terminals (Figure 5C; *SV2B*$^{-/-}{}_{\text{solutionA}}$: 112 ± 27 nM, n = 14; $WT_{\text{solutionC}}$: 117 ± 16 nM, n = 20; $WT_{\text{solution D}}$: 113 ± 16 nM, n = 5) and significantly higher than WT control (32 ± 6 nM, n = 12, one-way ANOVA with Dunnett Multiple Comparisons Test, p = 0.011). Furthermore, as shown in Figure 7A, dialysis with solution D fully mimicked the elevated train-evoked Ca^{2+} response of *SV2B*$^{-/-}$ neurons, while dialysis with solution C, which had a higher concentration of free EGTA (Table 1), had a Ca^{2+} profile that was intermediary between the WT and *SV2B*$^{-/-}$ Ca^{2+} phenotype.

What happens to exocytosis in WT terminals with an *SV2B*$^{-/-}$ Ca^{2+} phenotype? Figure 7B demonstrates that there was no difference in the amplitude of the first capacitance jump between WT neurons with a *SV2B*$^{-/-}$ Ca^{2+} phenotype ($WT_{\text{solutionC}}$: 9.3 ± 1.3fF, n = 21; $WT_{\text{solutionD}}$: 9.4 ± 0.5 fF, n = 5) and our standard

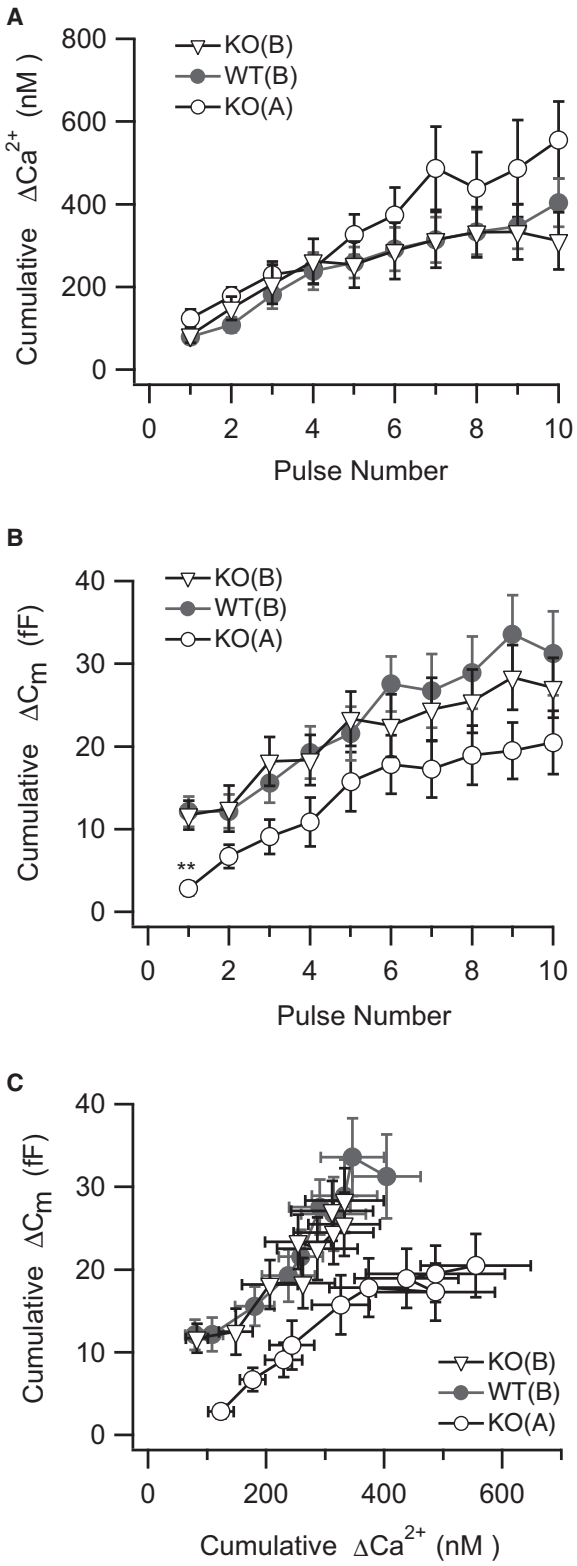

Figure 6. Restoration of Presynaptic Ca^{2+} Concentration to WT Levels Rescues the Secretory Phenotype of *SV2B*$^{-/-}$ Neurons

(A) Restoration of presynaptic Ca^{2+} concentration to WT levels for ≈2 min in *SV2B*$^{-/-}$ neurons with solution B [KO(B), open triangles] was sufficient to rescue the cumulative Ca^{2+} concentration response evoked by the pulse train. (B) When resting Ca^{2+} concentration was lowered in *SV2B*$^{-/-}$ neurons with solution B [KO(B), open triangles], the magnitude of the first C_m response became identical to that of WT littermates [WT(B), filled circles; one-way ANOVA, followed by Dunnett's Multiple Comparisons Test; **p < 0.01]. (C) Upon restoration of presynaptic Ca^{2+} concentration in *SV2B*$^{-/-}$ neurons to WT levels [KO(B), open triangles], the mean cumulative ΔCa^{2+} concentration as a function of the mean cumulative ΔC_m became superimposable onto that of WT neurons.
Error bars represent SEM.

solution A ($WT_{solutionA}$: 9.2 ± 1.5 fF, n = 13). All three differed from the amplitude of the first C_m jump in *SV2B*$^{-/-}$ neurons dialyzed with standard solution A (Figure 7B; 2.8 ± 0.8 fF, n = 12; one way ANOVA with Dunnett Multiple Comparisons Test, p = 0.0035). In addition, WT neurons with an *SV2B*$^{-/-}$ Ca^{2+} phenotype did not exhibit an apparent decrease in the calcium sensitivity of release (Figure 7C, PROC Mixed analysis, $WT_{solutionC}$-$WT_{solutionA}$: p = 0.21; $WT_{solutionD}$-$WT_{solutionA}$: p = 0.34; $WT_{solutionC}$-$KO_{solutionA}$: p < 0.0001; $WT_{solutionD}$-$KO_{solutionA}$: p < 0.0001). Thus, while elevated resting and evoked presynaptic Ca^{2+} reveals both the early secretory defect and the decrease in the apparent Ca^{2+}-sensitivity of release, short-term elevation of presynaptic Ca^{2+} of the type tested here is insufficient to trigger these changes.

Two aspects of the *SV2B*$^{-/-}$ secretory phenotype, however, were reproduced in WT neurons with an *SV2B*$^{-/-}$ Ca^{2+} phenotype. First, similar to what was observed in *SV2B*$^{-/-}$ neurons (Figure 7B), WT neurons with an *SV2B*$^{-/-}$ Ca^{2+} phenotype showed a significant early enhancement in the cumulative capacitance response that was reminiscent of *SV2B*$^{-/-}$ neurons (Slope $WT_{solutionD}$: 4.3 ± 0.02) and different from control WT neurons (Figure 3B; PROC Mixed analysis, slope $WT_{solutionA}$ versus slope $WT_{solutionD}$, p = 0.05). Second, following the stimulus train, the time constants of membrane recovery in WT neurons with an *SV2B*$^{-/-}$ Ca^{2+} phenotype were prolonged relative to WT controls (Figure 5D; $WT_{solutionA}$ 4.5 ± 0.9 s, n = 12; $WT_{solutionC}$: 9.1 ± 1.6 s, n = 11; $WT_{solutionD}$: 7.6 ± 2.1 s, n = 5), and approached values observed in *SV2B*$^{-/-}$ neurons (*SV2B*$^{-/-}$ $_{solutionA}$: 9.5 ± 0.8 s, n = 8). These results, together with those from the previous section, demonstrate that enhancement and membrane recovery are sensitive to the manipulation of presynaptic Ca^{2+} signaling in both directions. Thus, these two features of the *SV2B*$^{-/-}$ secretory phenotype are likely to be a direct consequence of the changes in presynaptic Ca^{2+} signaling associated with SV2 deficiency.

DISCUSSION

SV2B Regulates Presynaptic Ca^{2+}

We took advantage of the relatively large and accessible nerve terminal of the mouse rod bipolar neuron to make time-resolved quantitative measurements of presynaptic Ca^{2+} concentration from SV2-deficient and WT neurons. Our data provide a direct demonstration that an SV2 protein affects presynaptic Ca^{2+} signaling. The loss of SV2B, the major SV2 isoform expressed by rod bipolar cells, was associated with an increase in the basal Ca^{2+} concentration in rod bipolar cell nerve terminals and an increased accumulation of presynaptic Ca^{2+} during a stimulus

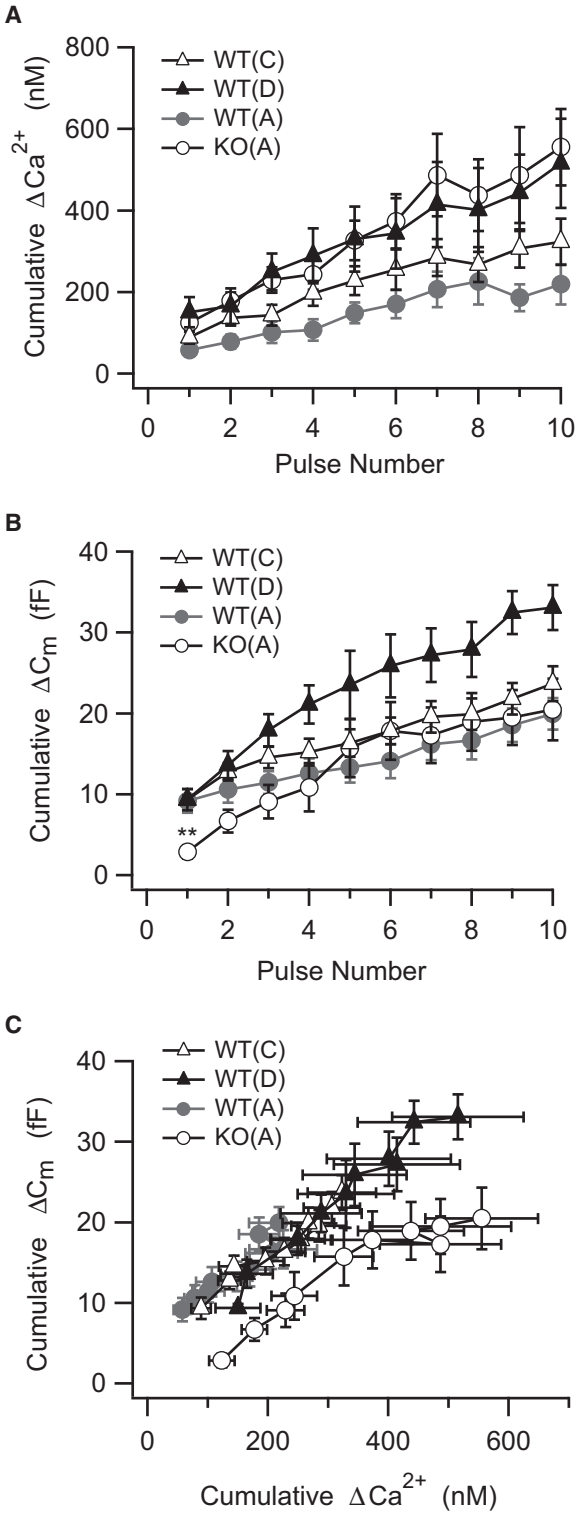

Figure 7. Replication of the *SV2B*$^{-/-}$ Ca^{2+} Phenotype in WT Neurons Does Not Reproduce the *SV2B*$^{-/-}$ Secretory Phenotype

(A) Elevation of the resting Ca^{2+} concentration in WT neurons to *SV2B*$^{-/-}$ (KO) levels with solution C for ≈2 min did not mimic the cumulative Ca^{2+} concentration phenotype [WT(C), open triangles]. However, when free EGTA in the high Ca^{2+} recording solution was reduced with solution D [WT(D), black triangles; see Table 1], the cumulative Ca^{2+} concentration record resembled that of *SV2B*$^{-/-}$ neurons [KO(A), open circles].

(B) Elevation of resting Ca^{2+} concentration in WT neurons [WT(C), open triangles] did not suppress the secretory response to the first pulse in the train relative to WT controls [WT(A), filled circles; one-way ANOVA, followed by Dunnett's Multiple Comparisons test; **$p < 0.01$].

(C) Elevation of presynaptic Ca^{2+} concentration, with or without a decrease in free EGTA [WT(C) and WT(D), respectively], failed to reproduce the rightward shift in the mean cumulative ΔC_m with respect to the mean cumulative ΔCa^{2+} concentration that was observed in *SV2B*$^{-/-}$ neurons.

Error bars represent SEM.

train. That these changes in Ca^{2+} concentration are consequential was evidenced by altered synaptic vesicle dynamics and dramatic changes in the pattern of neurotransmitter release. Our data extend previous studies that have hinted at a role for SV2 in the regulation of presynaptic Ca^{2+} based upon the action of an exogenous Ca^{2+} chelator (Chang and Südhof, 2009; Janz et al., 1999). While our results appear to contrast with a recent study in endocrine cells (Iezzi et al., 2005), it is important to note that in that particular study Ca^{2+} measurements were made with low temporal resolution and in response to strong stimulation. Thus, small differences in Ca^{2+} signaling that may have occurred on a fast timescale or in advance of the saturation of other Ca^{2+} handling mechanisms were unlikely to be detected.

How might SV2 proteins regulate presynaptic Ca^{2+}? SV2 proteins belong to a large superfamily of transporter molecules and contain two conserved negatively charged amino acids in the first transmembrane-spanning domain (Janz and Südhof, 1999). This has led to the hypothesis that SV2 proteins are Ca^{2+} transporters (Janz et al., 1999), moving Ca^{2+} ions from the cytosol into secretory vesicles, a compartment suggested to contain Ca^{2+} ions (Kendrick et al., 1977; Schmidt et al., 1980; Xin and Wightman, 1998). We estimate that SV2 could potentially provide at least 10,000 Ca^{2+} binding sites per bouton, assuming a conservative vesicle density per synaptic bouton in mouse rod bipolar cells approximately 1/5 that of the goldfish Mb1 bipolar terminal (von Gersdorff et al., 1996) and an average of two copies of SV2 per synaptic vesicle (Takamori et al., 2006). By contrast, the cumulative train-evoked ΔCa^{2+} in the *SV2B*$^{-/-}$ terminals was 337 nM higher than that of wild-type. For a single 3 μm bouton, this corresponds to ≈2869 additional free-Ca^{2+} ions. Thus, the number of Ca^{2+} binding sites afforded by SV2 molecules would be more than sufficient to account for the difference in stimulus-evoked free Ca^{2+}. In our experiments, loss of SV2 proteins had the most pronounced effect on Ca^{2+} within the interstimulus interval (250 ms). SV2 proteins might therefore serve as fast, high-affinity Ca^{2+} transporters or binding proteins.

SV2 proteins also could conceivably interact with voltage-gated Ca^{2+} channels or Ca^{2+} pumps to effect changes in Ca^{2+} signaling. However, the localization of SV2 in the synaptic vesicle membrane makes an interaction with plasma membrane Ca^{2+} channels or Ca^{2+} pumps, located on the plasma membrane, mitochondria and endoplasmic reticulum (Krizaj et al., 2002), unlikely. Furthermore, Ca^{2+} clearance following stimulation, dominated by plasma membrane Ca^{2+} pumps in rod-dominant bipolar cells (Zenisek and Matthews, 2000), was not affected by the loss of SV2B (Figure 4).

SV2 Deficiency Alters Ca^{2+}-Regulated Synaptic Vesicle Dynamics

There are multiple Ca^{2+}-regulated steps in the secretory pathway (Heidelberger, 2001; Neher and Sakaba, 2008). These include vesicle mobilization and the refilling of vesicle pools (Gomis et al., 1999; Mennerick and Matthews, 1996; Sakaba and Neher, 2001; von Rüden and Neher, 1993; Wang and Kaczmarek, 1998). In response to a stimulus train, rod bipolar cells lacking SV2B exhibited a secretory response that was initially suppressed but was followed by an enhancement that briefly converted depression to facilitation (Figure 3). These findings are congruent with the loss of enhancement and marked synaptic depression observed in cultured *SV2A/B*$^{-/-}$ neurons following treatment with an exogenous Ca^{2+}-buffer (Chang and Südhof, 2009; Janz et al., 1999). Enhancement was also observed in wild-type neurons with an SV2 Ca^{2+} phenotype (Figure 7). We therefore propose that altered presynaptic Ca^{2+} signaling underlies the pronounced changes in synaptic strength observed in SV2-deficient neurons.

Endocytosis is also Ca^{2+} regulated (Balaji et al., 2008; Ceccarelli and Hurlbut, 1980; Gad et al., 1998; Marks and McMahon, 1998; Sankaranarayanan and Ryan, 2001; Wu et al., 2009). In retinal bipolar cells, elevation of bulk presynaptic Ca^{2+} levels inhibits compensatory endocytosis (Rouze and Schwartz, 1998; von Gersdorff and Matthews, 1994; Wan et al., 2008). Here, we show that SV2B loss slows membrane recovery following a pulse train and that this is a direct consequence of the change in Ca^{2+} signaling attributable to SV2B loss (Figures 4 and 5). The mechanism underlying the Ca^{2+}-dependent slowing of endocytosis is not well understood; however, it does not appear to be caused by the saturation of the rod bipolar cell endocytotic machinery (Wan et al., 2008). Rather, it may relate to ongoing release following Ca^{2+} channel closure, inhibition of endocytosis by elevated Ca^{2+} (Rouze and Schwartz, 1998; von Gersdorff and Matthews, 1994), or changes in internal Cl^- resulting from activation of a Ca^{2+}-dependent Cl^- current (Hull and von Gersdorff, 2004). In this context, it is important to note that the slowing of membrane recovery is unlikely to have an immediate impact on pool refilling, as multiple rounds of release can occur in bipolar cells in the absence of endocytosis (Heidelberger et al., 2002; von Gersdorff and Matthews, 1997), presumably because these neurons refill the releasable pool from their unusually large reserve pool (von Gersdorff et al., 1996).

SV2 Is Required for Maintenance of the Rapidly Releasing Pool

We observed a pronounced exocytotic defect characterized by a reduction in vesicle fusion evoked by a single, nonsaturating depolarization and a decrease in the apparent Ca^{2+} sensitivity of release in *SV2B*$^{-/-}$ neurons (Figure 3). Both effects are in the range of 6–7 fF, a magnitude similar to that of the rapidly releasing pool of vesicles in rodent rod bipolar cells (Singer and Diamond, 2006; Wan et al., 2008). Given that there was no change in vesicle diameter or in the number of synaptic ribbons (Figure 1 and Table S1) and that the changes in presynaptic Ca^{2+} concentration were sufficient to evoke release, SV2 deficiency is most likely associated with a defect in the rapidly releasing pool. Similarly, a decrease in the number of secretory granules available for rapid release has been described in endocrine cells lacking SV2A (Xu and Bajjalieh, 2001), and in *SV2A/B*$^{-/-}$ cultured neurons, the amplitude of the first postsynaptic current evoked by a train was decreased (Chang and Südhof, 2009), potentially indicating a decrease in the number of vesicles available for release. Thus, SV2A and SV2B modulate the number or function of vesicles available for rapid release. Further, this role is conserved across large, dense-core secretory granules and small, clear-core synaptic vesicles. Interestingly, the total extent of exocytosis evoked by a stimulus train was comparable between WT controls and *SV2B*$^{-/-}$ neurons (Figure 3B), indicating that the build-up of presynaptic Ca^{2+} during the pulse train in SV2-deficient neurons and the consequent enhancement overcomes the defect.

SV2 proteins interact with synaptotagmin 1 (Bennett et al., 1992; Lazzell et al., 2004; Schivell et al., 1996, 2005), a Ca^{2+} sensor for fast exocytosis that is present in rod bipolar cell terminals (Heidelberger et al., 2003). Synaptotagmin is also important for the positional priming of synaptic vesicles and maintenance of vesicle pools (Young and Neher, 2009). This raises the possibility that the SV2-deficiency secretory phenotype results from altered synaptotagmin function. However, there is almost 10-fold more synaptotagmin on synaptic vesicles isolated from the brain than SV2 (Takamori et al., 2006). Thus, if the same ratio holds for synaptic vesicles of retinal ribbon synapses, the relevant synaptotagmin molecules must specifically be those that interact with SV2. However, this scenario does not readily account for the rescue of the *SV2B*$^{-/-}$ secretory phenotype upon restoration of presynaptic Ca^{2+} signaling to WT levels. One would need to postulate an additional action such as the presence of SV2 makes the release machinery less sensitive to Ca^{2+}-adaptation, an interesting hypothesis that warrants future investigation.

In some studies, a reduction in synaptotagmin levels has been described in SV2 deficient neurons (Morgans et al., 2009; Yao et al., 2010; but see Crowder et al., 1999; Janz et al., 1999). In *SV2B*$^{-/-}$ retinae, photoreceptor terminals, but not bipolar cells, show a decrease in synaptotagmin immunolabeling (Lazzell et al., 2004; Morgans et al., 2009). If the functional reduction in the rapidly releasing pool and the decrease in the apparent Ca^{2+} sensitivity of release were due to a loss of synaptotagmin in rod bipolar cells, lowering the *SV2B*$^{-/-}$ Ca^{2+} phenotype to wild-type levels should worsen the secretory defect. However, we observed the opposite effect (Figure 6). Furthermore, the rapidity with which the secretory defect was rescued upon lowering presynaptic Ca^{2+} to WT levels indicates that the synaptotagmin levels in the terminal could support normal secretion and is difficult to reconcile with a reduction in synaptotagmin concentration.

We can similarly rule out changes in the concentrations of other synaptic proteins as mediators of the SV2-deficiency secretory phenotype. In agreement with quantitative immunoblots performed on brains from *SV2A/B*$^{-/-}$ mice (Janz and Südhof, 1999), analysis of immunolabeling in *SV2B*$^{-/-}$ retinae did not reveal changes in the levels of other major synaptic vesicle proteins (Lazzell et al., 2004; Morgans et al., 2009). Morgans et al. (2009) did report reductions in synaptobrevin/VAMP, VGluT1, and synaptophysin in *SV2B*$^{-/-}$ mouse eye

extracts, but these reductions were not of a magnitude known to disrupt synaptic transmission (Fremeau et al., 2004; McMahon et al., 1996; Schoch et al., 2001; Wojcik et al., 2004). As with synaptotagmin, the rapid rescue of the secretory phenotype upon restoration of presynaptic Ca^{2+} signaling is difficult to reconcile with the reduction of a major vesicular protein.

The hypothesis most consistent with our data is that the role of SV2 in exocytosis is mediated via its ability to regulate presynaptic Ca^{2+}. Potentially, the increase in basal presynaptic Ca^{2+} concentration could trigger vesicle fusion (Lagnado et al., 1996), decreasing the number of vesicles available for stimulus-driven release (Wasser and Kavalali, 2009; Xu et al., 2009). However, although we observed an increase in capacitance fluctuations in *SV2B*$^{-/-}$ bipolar cells that might reflect an increase in spontaneous fusion and retrieval events (data not shown), our high Ca^{2+} recording solutions increased the spontaneous capacitance fluctuations of WT neurons to comparable levels without reproducing the secretory defect (Figure 7). In addition, cultured neurons from SV2-deficient mice exhibit a similar secretory defect in the absence of an increase in spontaneous release (Chang and Südhof, 2009; Crowder et al., 1999; Custer et al., 2006). Thus, simple, use-dependent exhaustion of the rapidly releasing pool is probably insufficient to account for the observed secretory defect.

A more likely explanation for the decrease in the rapidly releasing pool of vesicles and the decrease in the apparent Ca^{2+} sensitivity of release is adaptation induced by the chronic elevation of presynaptic Ca^{2+}. Elevated Ca^{2+} is a well-known stimulus for adaptation in neurons, including at the level of the release machinery (Eatock et al., 1987; Kline et al., 2007; Kurahashi and Shibuya, 1990; Wu et al., 2008). Chronic, mild stimulation has also been suggested to decrease vesicle priming and the number of vesicles available for release (Bélair et al., 2005; Millar et al., 2005; Moulder et al., 2006). Synaptic adaptation in the face of mild stimulation requires days rather than minutes (Molder et al., 2006), consistent with our inability to reproduce all aspects of the *SV2B*$^{-/-}$ secretory phenotype upon short-term doubling of the resting presynaptic Ca^{2+}. Our anatomical analyses of SV2-deficient neurons revealed no alteration in the number of synaptic ribbons and no gross deficiencies in the synaptic architecture. Presumably therefore, any adaptive modification associated with SV2 deficiency occurs at the molecular level, consistent with its rapid reversibility. This type of Ca^{2+}-dependent adaptation may play a critical role in the maintenance of synaptic homeostasis in the face of chronically enhanced Ca^{2+} associated with SV2 deficiency. Given that all aspects of the SV2-deficiency secretory phenotype are rapidly reversed upon restoration of the Ca^{2+} phenotype to that of WT controls, our results suggest that therapeutic regulation of presynaptic Ca^{2+} signaling and Ca^{2+}-accelerated vesicle supply are areas worthy of further exploration as potential interventions for some forms of epilepsy.

EXPERIMENTAL PROCEDURES

Animals

All animal procedures conformed to NIH guidelines and were approved by the Animal Welfare Committee of the University of Texas Health Science Center at Houston. The generation of the *SV2B*$^{-/-}$ mice has been previously described (Janz et al., 1999). The *SV2B*$^{-/-}$ mice were bred against C57BL/6 mice for at least six generations and were maintained as a heterozygous line. Matching *SV2B*$^{-/-}$ and WT animals were generated by heterozygous interbreeding. Animals were genotyped using PCR as described (Janz et al., 1999). The person performing the electrophysiology had no knowledge of the genotype of the animals used during the experiment.

Cell Isolation

Rod bipolar neurons were isolated from the retinas of 2- to 6-month-old C57BL/6 and *SV2B*$^{-/-}$ mice by enzymatic digestion followed by mechanical trituration as described previously (Wan et al., 2008; Zhou et al., 2006). Isolated rod bipolar neurons were identified and selected for recording based on morphological criteria as previously described (Zhou et al., 2006).

Electron Microscopy and Measurement of Vesicle Size

Following euthanasia of wild-type or *SV2B*$^{-/-}$ mice, eyeballs were rapidly enucleated, and the anterior segment was removed. The resulting eyecups were fixed in 2% paraformaldehyde + 2% glutaraldehyde in 0.1 M cacodylate buffer (pH 7.2) overnight at 4°C. Eyecups were postfixed in 1% OsO_4 for 1 hr at 4°C, dehydrated through 50%–100% ethanol followed by propylene oxide and embedded in LX112-araldite epoxy resin (Ladd Research Industries, Williston, VT). Thin sections of gold interference color (~150 nm thickness) were collected onto copper grids, poststained with lead citrate and uranyl acetate, and examined using a transmission electron microscope (Technai G2 Biotwin, FEI, Hillsboro, OR; or H-7600, Hitachi, Tokyo, Japan). To analyze synaptic structure and vesicle size, images of bipolar cell terminals in wild-type and SV2B knockout retinas were imaged digitally at 20,000×–50,000×. Images were imported into NIH ImageJ and image scale was calibrated. Individual vesicles were traced manually along their outer circumference and the following variables were measured: vesicle area (nm^2), vesicle perimeter (nm), major axis and minor axis (determined by the best-fit ellipse), and the maximum diameter of the vesicle (Feret's diameter). The synaptic vesicle diameters measured in our studies are similar to the synaptic vesicle diameter reported previously for mouse rod bipolar cells (Spiwoks-Becker et al., 2001) and slightly larger than the diameter reported for synaptic vesicles in goldfish Mb bipolar cell terminals (von Gersdorff et al., 1996). The small differences in vesicle sizes observed across these studies likely arise from differences in fixation, tissue processing, and embedding media. We also calculated an adjusted Feret's diameter using Abercrombie's correction factor to compensate for systematic underestimation of objects that can occur in thin sections (Abercrombie, 1946). Statistical comparisons were performed using Student's two-tailed t test for unpaired samples. The criterion for statistical significance was set at $p < 0.05$.

Immunocytochemistry and Imaging

Freshly isolated *SV2B*$^{-/-}$ mouse retinal cells were deposited onto glass coverslips coated with 0.1 mg/ml poly-D-lysine and allowed to settle for 15 min. The cells were washed in 0.1 M phosphate buffer (PB), fixed in 4% paraformaldehyde for 15 min at RT, and then rinsed. Cells were incubated in primary antibodies diluted in 1% normal goat serum in PB for 24 hr at 4°C. To positively identify synaptic ribbons in rod bipolar cells, isolated cells were labeled simultaneously using a mouse monoclonal antibody against the synaptic ribbon marker, CtBP2/Ribeye (1:200; BD Transduction Laboratories, San Jose, CA) and a rabbit polyclonal antiserum against the rod bipolar cell marker PKC-α (1:1000; Calbiochem, San Diego, CA). Secondary antisera specific for rabbit or mouse immunoglobulins were raised in goat and were conjugated to either AlexaFluor 568 or AlexaFluor 488 (1:1000 dilution; Molecular Probes, Eugene, OR). Immunolabeling was imaged with a Zeiss Laser Scanning Microscope 510 META (Zeiss, Thornwood, NY) using either Plan Apochromat 63× (1.4 NA) or Plan Neofluar 40× (1.3 NA) oil-immersion objective lenses. Images in the two fluorescent channels were collected sequentially and laser power and detector sensitivity were adjusted to prevent spectral bleed-through during image acquisition. To determine the number of synaptic ribbons in rod bipolar cell terminals of cells isolated from WT and *SV2B*$^{-/-}$ retina, short stacks of optical sections through the terminals of PKC-α-positive rod bipolar cells were acquired (typically six optical sections at a step size of 0.2 μm) to

ensure that individual ribbons were only counted once. Image stacks were compressed into a maximum intensity projection, and the number of synaptic ribbons in rod bipolar cell terminals was determined by counting the number of CtBP2-positive fluorescent puncta within the PKCα-positive terminals.

Electrophysiological and Intraterminal Ca^{2+} Measurements

All experiments were performed at room temperature (~25°C). Whole-cell recordings from the soma of intact rod bipolar neurons were performed with a 5–6 MΩ pipette pulled from borosilicate glass using a Sutter Instruments P-97 puller (Novato, CA, USA). Electrophysiological and capacitance measurements were made using an EPC-9 patch-clamp amplifier controlled via PULSE LOCK-IN software (HEKA Electroniks, Lambrecht, Germany). To monitor membrane capacitance, a 30 mV peak-to-peak, 800 Hz sinusoidal voltage command was applied about the holding potential of −70 mV, and the resultant signal was processed by the Lindau-Neher technique to calculate C_m, G_m, and G_s (Wan et al., 2008; Zhou et al., 2006). For time-resolved capacitance measurements, one capacitance point was generated per each 100 ms sweep. For high-resolution capacitance measurements during the train, one capacitance data point was generated per sine-wave cycle. Briefly, a 4 Hz train of ten 100 ms depolarizing pulses (−70 to 0 mV) was given (Figure S1). Five ms after each depolarizing pulse, a 50 ms sinusoidal voltage command was superimposed over the holding potential of −70 mV. The first 25 ms interval following the 100 ms depolarization was excluded from analysis due to potential complications associated with gating currents and/or the decay of depolarization evoked conductance changes (Gillis, 1995; Horrigan and Bookman, 1994; Wan et al., 2008). The mean capacitance value for each depolarization in the train was determined from the average capacitance value of the remaining 30 ms period.

The standard external recording solution contained (in mM) 127 NaCl, 5 CsCl, 20 TEA-Cl, 1 $MgCl_2$, 2 $CaCl_2$, 10 glucose, and 10 HEPES, pH = 7.4, 315–320 mOsm. Unless noted, recordings were made using the standard intracellular solution (Table 1, solution A) which contained (in mM) 125 Cs-gluconate, 10 TEA-Cl, 3 $MgCl_2$, 2 Na_2ATP, 0.5 GTP, 0.5 EGTA, 0.2 bis-fura-2, 35 HEPES, pH = 7.2, 310–315 mOsm. Additional intracellular solutions used to clamp presynaptic Ca^{2+} and free EGTA to specific concentrations are defined in Table 1. To ensure that terminals were fully dialyzed with the intracellular solution, we allowed at least 2 min for the bis-fura-2 fluorescence signal to reach a plateau before presenting the first stimulus. Intraterminal Ca^{2+} measurements were performed using a computer-controlled monochrometer-based system (ASI/TILL Photonics, Eugene, OR; Messler et al., 1996). Intraterminal Ca^{2+} concentration was determined from the ratio of the fluorescence signals excited at 340 and 380 nm, using calibration constants obtained as described previously (Heidelberger and Matthews, 1992). An adjustable aperture was used to position the collection field for emitted fluorescence selectively over the terminal (Wan et al., 2008; Zhou et al., 2006).

Data Analysis

Cells with leak currents larger than 30 pA or access resistances >35 MΩ were excluded from analysis. Cells were also excluded if changes in C_m were correlated with changes in membrane conductance (G_m) and series conductance (G_s). Data analysis was performed using IGOR Pro software (Wavemetrics, Lake Oswego, OR, USA). Results are presented as mean ± SEM. To calculate the cumulative ΔC_m, the membrane capacitance after each depolarization pulse was subtracted from the resting C_m, which was defined as the average C_m value over the 5 s period immediately before the first depolarization. To calculate cumulative ΔCa^{2+}, the Ca^{2+} concentration immediately after each depolarization pulse was subtracted from the resting Ca^{2+} concentration, which was defined as the average Ca^{2+} concentration over the 5 s period immediately before the first depolarizing stimulus pulse. To measure the rate of membrane recovery, for each record, the falling phase of the capacitance response was fit with a single exponential function (Wan et al., 2008).

Statistical comparisons were performed using the two-tailed, unpaired Student's t-test or one-way ANOVA with Dunnett's Multiple Comparisons Test (Sigmaplot 11.0 software, Access Softek, San Jose, CA, USA), unless indicated otherwise. To estimate the effects of mean cumulative ΔCa^{2+} on mean cumulative ΔC_m among groups, an analysis of covariance with repeated-measurements (PROC Mixed) was performed using SAS for Windows 9.1 software (SAS Institute, Cary, NC). The dependent variable was the mean cumulative ΔC_m and independent variables were the mean cumulative ΔCa^{2+}, group, and intergroup interaction. If the effect of the interaction term was not significant, it indicated that the slopes of linear trend did not differ among the groups and a model with different intercepts and same slope was further studied. PROC Mixed analysis with a repeated-measurement model was used to estimate the slope of the mean cumulative ΔC_m during the initial 3 pulses of the train among groups. Statistical significance was set at $p \leq 0.05$.

SUPPLEMENTAL INFORMATION

Supplemental Information includes one figure and one table and can be found with this article online at doi:10.1016/j.neuron.2010.05.010.

ACKNOWLEDGMENTS

This work was supported by National Eye Institute Grant EY-12128 to R.H., EY-16452 to R.J., and Core Grant EY-10608. We thank Dr. Alice Z. Chuang for her assistance with the statistical analysis and Margaret Gondo and Joe Wilkerson for technical assistance with electron microscopy. Electron microscopy at the University of Houston was supported by an NIH CORE grant to the University of Houston College of Optometry (P30 EY07751). Electron microscopy at the University of Oklahoma Health Sciences Center was performed at the Oklahoma Medical Research Foundation Imaging Core Facility. Q.-F.W., Z.-Y.Z., P.T., D.M.S., R.J., and R.H. contributed to the design and interpretation of the experiments. Q.-F.W., Z.-Y.Z., and P.T. conducted the electrophysiological experiments. A.V. and P.T. performed the immunocytochemistry. D.M.S. performed the electron microscopy. R.H., Q.-F.W., and R.J. wrote the manuscript. R.H. and R.J. supervised the project. All authors have approved the manuscript.

Accepted: May 6, 2010
Published: June 23, 2010

REFERENCES

Abercrombie, M. (1946). Estimation of nuclear population from microtome sections. Anat. Rec. (Hoboken) *94*, 239–247.

Bajjalieh, S.M., Peterson, K., Shinghal, R., and Scheller, R.H. (1992). SV2, a brain synaptic vesicle protein homologous to bacterial transporters. Science *257*, 1271–1273.

Bajjalieh, S.M., Frantz, G.D., Weimann, J.M., McConnell, S.K., and Scheller, R.H. (1994). Differential expression of synaptic vesicle protein 2 (SV2) isoforms. J. Neurosci. *14*, 5223–5235.

Balaji, J., Armbruster, M., and Ryan, T.A. (2008). Calcium control of endocytic capacity at a CNS synapse. J. Neurosci. *28*, 6742–6749.

Bélair, E.L., Vallée, J., and Robitaille, R. (2005). Long-term in vivo modulation of synaptic efficacy at the neuromuscular junction of Rana pipiens frogs. J. Physiol. *569*, 163–178.

Bennett, M.K., Calakos, N., and Scheller, R.H. (1992). Syntaxin: a synaptic protein implicated in docking of synaptic vesicles at presynaptic active zones. Science *257*, 255–259.

Buckley, K., and Kelly, R.B. (1985). Identification of a transmembrane glycoprotein specific for secretory vesicles of neural and endocrine cells. J. Cell Biol. *100*, 1284–1294.

Ceccarelli, B., and Hurlbut, W.P. (1980). Ca^{2+}-dependent recycling of synaptic vesicles at the frog neuromuscular junction. J. Cell Biol. *87*, 297–303.

Chang, W.P., and Südhof, T.C. (2009). SV2 renders primed synaptic vesicles competent for Ca^{2+} -induced exocytosis. J. Neurosci. *29*, 883–897.

Crowder, K.M., Gunther, J.M., Jones, T.A., Hale, B.D., Zhang, H.Z., Peterson, M.R., Scheller, R.H., Chavkin, C., and Bajjalieh, S.M. (1999). Abnormal neurotransmission in mice lacking synaptic vesicle protein 2A (SV2A). Proc. Natl. Acad. Sci. USA *96*, 15268–15273.

Custer, K.L., Austin, N.S., Sullivan, J.M., and Bajjalieh, S.M. (2006). Synaptic vesicle protein 2 enhances release probability at quiescent synapses. J. Neurosci. *26*, 1303–1313.

De Smedt, T., Raedt, R., Vonck, K., and Boon, P. (2007). Levetiracetam: the profile of a novel anticonvulsant drug-part I: preclinical data. CNS Drug Rev. *13*, 43–56.

Dong, M., Yeh, F., Tepp, W.H., Dean, C., Johnson, E.A., Janz, R., and Chapman, E.R. (2006). SV2 is the protein receptor for botulinum neurotoxin A. Science *312*, 592–596.

Dong, M., Liu, H., Tepp, W.H., Johnson, E.A., Janz, R., and Chapman, E.R. (2008). Glycosylated SV2A and SV2B mediate the entry of botulinum neurotoxin E into neurons. Mol. Biol. Cell *19*, 5226–5237.

Dowling, J.E. (1968). Synaptic organization of the frog retina: an electron microscopic analysis comparing the retinas of frogs and primates. Proc. R Soc. Lond. B Biol. Sci. *170*, 205–228.

Eatock, R.A., Corey, D.P., and Hudspeth, A.J. (1987). Adaptation of mechanoelectrical transduction in hair cells of the bullfrog's sacculus. J. Neurosci. *7*, 2821–2836.

Feany, M.B., Lee, S., Edwards, R.H., and Buckley, K.M. (1992). The synaptic vesicle protein SV2 is a novel type of transmembrane transporter. Cell *70*, 861–867.

Feng, G., Xiao, F., Lu, Y., Huang, Z., Yuan, J., Xiao, Z., Xi, Z., and Wang, X. (2009). Down-regulation synaptic vesicle protein 2A in the anterior temporal neocortex of patients with intractable epilepsy. J. Mol. Neurosci. *39*, 354–359.

Fremeau, R.T., Jr., Kam, K., Qureshi, T., Johnson, J., Copenhagen, D.R., Storm-Mathisen, J., Chaudhry, F.A., Nicoll, R.A., and Edwards, R.H. (2004). Vesicular glutamate transporters 1 and 2 target to functionally distinct synaptic release sites. Science *304*, 1815–1819.

Gad, H., Löw, P., Zotova, E., Brodin, L., and Shupliakov, O. (1998). Dissociation between Ca^{2+}-triggered synaptic vesicle exocytosis and clathrin-mediated endocytosis at a central synapse. Neuron *21*, 607–616.

Gillis, K.D. (1995). Techniques for membrane capacitance measurements. In Single-Channel Recording, B.S.E. Neher, ed. (New York, London: Plenum Press), pp. 155–198.

Gomis, A., Burrone, J., and Lagnado, L. (1999). Two actions of calcium regulate the supply of releasable vesicles at the ribbon synapse of retinal bipolar cells. J. Neurosci. *19*, 6309–6317.

Heidelberger, R. (2001). Electrophysiological approaches to the study of neuronal exocytosis and synaptic vesicle dynamics. Rev. Physiol. Biochem. Pharmacol. *143*, 1–80.

Heidelberger, R., and Matthews, G. (1992). Calcium influx and calcium current in single synaptic terminals of goldfish retinal bipolar neurons. J. Physiol. *447*, 235–256.

Heidelberger, R., Zhou, Z.Y., and Matthews, G. (2002). Multiple components of membrane retrieval in synaptic terminals revealed by changes in hydrostatic pressure. J. Neurophysiol. *88*, 2509–2517.

Heidelberger, R., Wang, M.M., and Sherry, D.M. (2003). Differential distribution of synaptotagmin immunoreactivity among synapses in the goldfish, salamander, and mouse retina. Vis. Neurosci. *20*, 37–49.

Horrigan, F.T., and Bookman, R.J. (1994). Releasable pools and the kinetics of exocytosis in adrenal chromaffin cells. Neuron *13*, 1119–1129.

Hull, C., and von Gersdorff, H. (2004). Fast endocytosis is inhibited by GABA-mediated chloride influx at a presynaptic terminal. Neuron *44*, 469–482.

Iezzi, M., Theander, S., Janz, R., Loze, C., and Wollheim, C.B. (2005). SV2A and SV2C are not vesicular Ca^{2+} transporters but control glucose-evoked granule recruitment. J. Cell Sci. *118*, 5647–5660.

Janz, R., and Südhof, T.C. (1999). SV2C is a synaptic vesicle protein with an unusually restricted localization: anatomy of a synaptic vesicle protein family. Neuroscience *94*, 1279–1290.

Janz, R., Hofmann, K., and Südhof, T.C. (1998). SVOP, an evolutionarily conserved synaptic vesicle protein, suggests novel transport functions of synaptic vesicles. J. Neurosci. *18*, 9269–9281.

Janz, R., Goda, Y., Geppert, M., Missler, M., and Südhof, T.C. (1999). SV2A and SV2B function as redundant Ca^{2+} regulators in neurotransmitter release. Neuron *24*, 1003–1016.

Kendrick, N.C., Blaustein, M.P., Fried, R.C., and Ratzlaff, R.W. (1977). ATP-dependent calcium storage in presynaptic nerve terminals. Nature *265*, 246–248.

Kline, D.D., Ramirez-Navarro, A., and Kunze, D.L. (2007). Adaptive depression in synaptic transmission in the nucleus of the solitary tract after in vivo chronic intermittent hypoxia: evidence for homeostatic plasticity. J. Neurosci. *27*, 4663–4673.

Krizaj, D., Demarco, S.J., Johnson, J., Strehler, E.E., and Copenhagen, D.R. (2002). Cell-specific expression of plasma membrane calcium ATPase isoforms in retinal neurons. J. Comp. Neurol. *451*, 1–21.

Kurahashi, T., and Shibuya, T. (1990). $Ca^{2(+)}$-dependent adaptive properties in the solitary olfactory receptor cell of the newt. Brain Res. *515*, 261–268.

Lagnado, L., Gomis, A., and Job, C. (1996). Continuous vesicle cycling in the synaptic terminal of retinal bipolar cells. Neuron *17*, 957–967.

Lazzell, D.R., Belizaire, R., Thakur, P., Sherry, D.M., and Janz, R. (2004). SV2B regulates synaptotagmin 1 by direct interaction. J. Biol. Chem. *279*, 52124–52131.

Lynch, B.A., Lambeng, N., Nocka, K., Kensel-Hammes, P., Bajjalieh, S.M., Matagne, A., and Fuks, B. (2004). The synaptic vesicle protein SV2A is the binding site for the antiepileptic drug levetiracetam. Proc. Natl. Acad. Sci. USA *101*, 9861–9866.

Mahrhold, S., Rummel, A., Bigalke, H., Davletov, B., and Binz, T. (2006). The synaptic vesicle protein 2C mediates the uptake of botulinum neurotoxin A into phrenic nerves. FEBS Lett. *580*, 2011–2014.

Marks, B., and McMahon, H.T. (1998). Calcium triggers calcineurin-dependent synaptic vesicle recycling in mammalian nerve terminals. Curr. Biol. *8*, 740–749.

McMahon, H.T., Bolshakov, V.Y., Janz, R., Hammer, R.E., Siegelbaum, S.A., and Südhof, T.C. (1996). Synaptophysin, a major synaptic vesicle protein, is not essential for neurotransmitter release. Proc. Natl. Acad. Sci. USA *93*, 4760–4764.

Mennerick, S., and Matthews, G. (1996). Ultrafast exocytosis elicited by calcium current in synaptic terminals of retinal bipolar neurons. Neuron *17*, 1241–1249.

Messler, P., Harz, H., and Uhl, R. (1996). Instrumentation for multiwavelengths excitation imaging. J. Neurosci. Methods *69*, 137–147.

Millar, A.G., Zucker, R.S., Ellis-Davies, G.C., Charlton, M.P., and Atwood, H.L. (2005). Calcium sensitivity of neurotransmitter release differs at phasic and tonic synapses. J. Neurosci. *25*, 3113–3125.

Morgans, C.W., Kensel-Hammes, P., Hurley, J.B., Burton, K., Idzerda, R., McKnight, G.S., and Bajjalieh, S.M. (2009). Loss of the Synaptic Vesicle Protein SV2B results in reduced neurotransmission and altered synaptic vesicle protein expression in the retina. PLoS ONE *4*, e5230.

Moulder, K.L., Jiang, X., Taylor, A.A., Olney, J.W., and Mennerick, S. (2006). Physiological activity depresses synaptic function through an effect on vesicle priming. J. Neurosci. *26*, 6618–6626.

Naraghi, M., and Neher, E. (1997). Linearized buffered Ca^{2+} diffusion in microdomains and its implications for calculation of $[Ca^{2+}]$ at the mouth of a calcium channel. J. Neurosci. *17*, 6961–6973.

Neher, E., and Sakaba, T. (2008). Multiple roles of calcium ions in the regulation of neurotransmitter release. Neuron *59*, 861–872.

Rouze, N.C., and Schwartz, E.A. (1998). Continuous and transient vesicle cycling at a ribbon synapse. J. Neurosci. *18*, 8614–8624.

Saier, M.H., Jr., Beatty, J.T., Goffeau, A., Harley, K.T., Heijne, W.H., Huang, S.C., Jack, D.L., Jähn, P.S., Lew, K., Liu, J., et al. (1999). The major facilitator superfamily. J. Mol. Microbiol. Biotechnol. *1*, 257–279.

Sakaba, T., and Neher, E. (2001). Calmodulin mediates rapid recruitment of fast-releasing synaptic vesicles at a calyx-type synapse. Neuron *32*, 1119–1131.

Sankaranarayanan, S., and Ryan, T.A. (2001). Calcium accelerates endocytosis of vSNAREs at hippocampal synapses. Nat. Neurosci. *4*, 129–136.

Schivell, A.E., Batchelor, R.H., and Bajjalieh, S.M. (1996). Isoform-specific, calcium-regulated interaction of the synaptic vesicle proteins SV2 and synaptotagmin. J. Biol. Chem. *271*, 27770–27775.

Schivell, A.E., Mochida, S., Kensel-Hammes, P., Custer, K.L., and Bajjalieh, S.M. (2005). SV2A and SV2C contain a unique synaptotagmin-binding site. Mol. Cell. Neurosci. *29*, 56–64.

Schmidt, R., Zimmermann, H., and Whittaker, V.P. (1980). Metal ion content of cholinergic synaptic vesicles isolated from the electric organ of Torpedo: effect of stimulation-induced transmitter release. Neuroscience *5*, 625–638.

Schoch, S., Deák, F., Königstorfer, A., Mozhayeva, M., Sara, Y., Südhof, T.C., and Kavalali, E.T. (2001). SNARE function analyzed in synaptobrevin/VAMP knockout mice. Science *294*, 1117–1122.

Singer, J.H., and Diamond, J.S. (2006). Vesicle depletion and synaptic depression at a mammalian ribbon synapse. J. Neurophysiol. *95*, 3191–3198.

Spiwoks-Becker, I., Vollrath, L., Seeliger, M.W., Jaissle, G., Eshkind, L.G., and Leube, R.E. (2001). Synaptic vesicle alterations in rod photoreceptors of synaptophysin-deficient mice. Neuroscience *107*, 127–142.

Takamori, S., Holt, M., Stenius, K., Lemke, E.A., Grønborg, M., Riedel, D., Urlaub, H., Schenck, S., Brügger, B., Ringler, P., et al. (2006). Molecular anatomy of a trafficking organelle. Cell *127*, 831–846.

von Gersdorff, H., and Matthews, G. (1994). Inhibition of endocytosis by elevated internal calcium in a synaptic terminal. Nature *370*, 652–655.

von Gersdorff, H., and Matthews, G. (1997). Depletion and replenishment of vesicle pools at a ribbon-type synaptic terminal. J. Neurosci. *17*, 1919–1927.

von Gersdorff, H., Vardi, E., Matthews, G., and Sterling, P. (1996). Evidence that vesicles on the synaptic ribbon of retinal bipolar neurons can be rapidly released. Neuron *16*, 1221–1227.

von Rüden, L., and Neher, E. (1993). A Ca-dependent early step in the release of catecholamines from adrenal chromaffin cells. Science *262*, 1061–1065.

Wan, Q.F., Vila, A., Zhou, Z.Y., and Heidelberger, R. (2008). Synaptic vesicle dynamics in mouse rod bipolar cells. Vis. Neurosci. *25*, 523–533.

Wang, L.Y., and Kaczmarek, L.K. (1998). High-frequency firing helps replenish the readily releasable pool of synaptic vesicles. Nature *394*, 384–388.

Wang, M.M., Janz, R., Belizaire, R., Frishman, L.J., and Sherry, D.M. (2003). Differential distribution and developmental expression of synaptic vesicle protein 2 isoforms in the mouse retina. J. Comp. Neurol. *460*, 106–122.

Wasser, C.R., and Kavalali, E.T. (2009). Leaky synapses: regulation of spontaneous neurotransmission in central synapses. Neuroscience *158*, 177–188.

Wojcik, S.M., Rhee, J.S., Herzog, E., Sigler, A., Jahn, R., Takamori, S., Brose, N., and Rosenmund, C. (2004). An essential role for vesicular glutamate transporter 1 (VGLUT1) in postnatal development and control of quantal size. Proc. Natl. Acad. Sci. USA *101*, 7158–7163.

Wu, W.W., Chan, C.S., Surmeier, D.J., and Disterhoft, J.F. (2008). Coupling of L-type Ca^{2+} channels to KV7/KCNQ channels creates a novel, activity-dependent, homeostatic intrinsic plasticity. J. Neurophysiol. *100*, 1897–1908.

Wu, X.S., McNeil, B.D., Xu, J., Fan, J., Xue, L., Melicoff, E., Adachi, R., Bai, L., and Wu, L.G. (2009). $Ca(^{2+})$ and calmodulin initiate all forms of endocytosis during depolarization at a nerve terminal. Nat. Neurosci. *12*, 1003–1010.

Xin, Q., and Wightman, R.M. (1998). Simultaneous detection of catecholamine exocytosis and Ca^{2+} release from single bovine chromaffin cells using a dual microsensor. Anal. Chem. *70*, 1677–1681.

Xu, T., and Bajjalieh, S.M. (2001). SV2 modulates the size of the readily releasable pool of secretory vesicles. Nat. Cell Biol. *3*, 691–698.

Xu, J., Pang, Z.P., Shin, O.H., and Südhof, T.C. (2009). Synaptotagmin-1 functions as a Ca^{2+} sensor for spontaneous release. Nat. Neurosci. *12*, 759–766.

Yao, J., Nowack, A., Kensel-Hammes, P., Gardner, R.G., and Bajjalieh, S.M. (2010). Cotrafficking of SV2 and synaptotagmin at the synapse. J. Neurosci. *30*, 5569–5578.

Young, S.M., Jr., and Neher, E. (2009). Synaptotagmin has an essential function in synaptic vesicle positioning for synchronous release in addition to its role as a calcium sensor. Neuron *63*, 482–496.

Zenisek, D., and Matthews, G. (2000). The role of mitochondria in presynaptic calcium handling at a ribbon synapse. Neuron *25*, 229–237.

Zhou, Z.Y., Wan, Q.F., Thakur, P., and Heidelberger, R. (2006). Capacitance measurements in the mouse rod bipolar cell identify a pool of releasable synaptic vesicles. J. Neurophysiol. *96*, 2539–2548.